Miklós KUCZMANN

"Széchenyi István" University

Measurement and simulation of vector hysteresis

Abstract. *The paper presents a rotational single sheet tester (RSST) which can be used to measure vector hysteresis characteristics inside a specimen with round shape. The measured hysteresis characteristics in the orthogonal directions presents uniaxial anisotropy. It has been handled by the Fourier expansion of the measured Everett functions. The Fourier coefficients of the unknown Everett function have been identified by the modification of a previously implemented algorithm. In the identification task linearly and circularly polarized measured data have been taken into account.*

Streszczenie. *Artykuł przedstawia obrotowy tester jedno-arkuszowy (RSST), który może być wykorzystany do pomiaru wektora histerezy w obiekcie o kształcie okrągłym. Mierzona w prostopadłych kierunkach pętla histerezy posiada jednoosiową anizotropię. Problem został rozwiązany przez użycie rozwinięcia Fouriera pomierzonych funkcji Everetta. Współczynniki Fouriera nieznanej funkcji Everetta zostały zidentyfikowane poprzez modyfikację zaimplementowanego algorytmu. W zadaniu identyfikacji wzięto pod uwagę liniowo i kołowo spolaryzowane dane pomiarowe. (**Pomiar i symulacja wektora histerezy**)*

Keywords: Everett function, Preisach model, Vector hysteresis characteristics.
Słowa kluczowe: funkcja Everetta, model Preisacha, charakterystyka wektora histerezy

Introduction

Different types of single sheet testers have been designed and manufactured to measure vector hysteresis properties of soft magnetic materials [1-10]. The Rotational Single Sheet Tester with a specimen with round shape (R-RSST) has been used in this study [9-10].

The Preisach model of hysteresis is the most widely applied simulation technique to approximate measured hysteresis curves [11,12]. The vector Preisach model is able to simulate vector behaviors of the field quantities inside the materials under test [11], i.e. the phase lag between the magnetic field intensity vector and the magnetic flux density vector is depending on the magnetization state. Either isotropic or anisotropic magnetic materials can be simulated by the vector Preisach model [11,13,14].

The identification of the vector Preisach model is a difficult task which is based on an integral equation and the Preisach distribution function [13] or the Everett function [14]. Very accurate results can be reached by the identification tasks.

However, the rotational properties of the vector hysteresis models are not always accurate enough. In the measurements, in the case of rotational magnetic flux density the magnetic field intensity vector does not follow a circular shape but a flower-like shape which can not be simulated by the original models [11,14]. This property is originated from some anisotropy of the material under test. The flower shaped magnetic field intensity can be reached by introducing a parameter which can be identified by applying some data from rotational measurements [15,16].

In this paper, a new vector Preisach model of magnetic hysteresis is presented which models accurately the anisotropic properties of the material as well as the rotational magnetization process.

The measured vector hysteresis characteristics

The RRSST system is an induction motor, which rotor has been removed and the round shaped specimen has been installed in this place. The block diagram of the measurement set-up can be seen in Fig. 1, the complete description is presented in [9,10]. The magnetic field inside the specimen can be generated by a special two-phase winding. The two orthogonal components of the magnetic field intensity $\boldsymbol{H}(t)$ or the magnetic flux density $\boldsymbol{B}(t)$ can be controlled by two independent current generators and an application developed in the frame of LabVIEW. The two orthogonal components of $\boldsymbol{H}(t)$ and of $\boldsymbol{B}(t)$ inside the specimen can be measured by a sensor system.

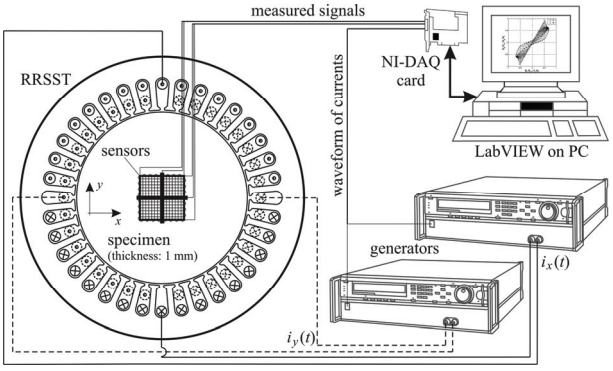

Fig.1. The vector hysteresis measurement system

The measured concentric minor loops and the corresponding Everett functions can be seen in Fig. 2. The magnetic flux density has been controlled to be sinusoidal, with preliminarily defined amplitude, to reach as small eddy current effect as possible. The meaning of Everett function will be shown in the next section, anyway, the measured hysteresis curves and the Everett function are identical from the simulation point of view.

First, the sample has been magnetized in the *x*, than in the perpendicular *y* direction, i.e. linear excitation has been supplied. The hysteresis characteristics measured in the *x* and in the *y* directions are almost the same as it can be seen in Fig. 2. The material has small uniaxial anisotropy, the *x* direction is the easy axis, and the *y* direction is the hard axis. This property has been taken into account. The material is basically isotropic, but the sample has been manufactured by a rolling technology, and the rolling direction is identical with the *x* direction.

In the followings, the inverse hysteresis characteristics are applied to build up the vector model, i.e. the input and the output of the system is the magnetic flux density and the magnetic field intensity, respectively. This is the reason why the Everett functions have the unusual shape. Moreover, the Everett functions are mirrored to the line $\beta=\alpha$ to approximate smoother derivatives of the Everett functions with respect to α and β.

The following elliptical interpolation has been supposed to approximate the smooth angular behavior of the Everett function [14]:

$$(1)\quad F(\alpha,\beta,\varphi)=\sqrt{F_x^2(\alpha,\beta)\cos^2\varphi+F_y^2(\alpha,\beta)\sin^2\varphi}\,,$$

where $F_x(\alpha,\beta)$ and $F_y(\alpha,\beta)$ are the measured Everett functions in the *x* and the perpendicular *y* directions, i.e. $F_x(\alpha,\beta)=F(\alpha,\beta,0)$, and $F_y(\alpha,\beta)=F(\alpha,\beta,\pi/2)$. The *x* and *y* directions are represented by the polar angle φ=0 and $\varphi=\pi/2$, respectively.

The measured Everett function is π-periodic, and it is an even function with respect to φ, i.e.

(2) $$F(\alpha,\beta,\varphi+\pi)=F(\alpha,\beta,\varphi)$$

and

(3) $$F(\alpha,\beta,-\varphi)=F(\alpha,\beta,\varphi)\ .$$

Due to the periodicity of the measured Everett function, it can be approximated by its Fourier series, which is presented in the next section.

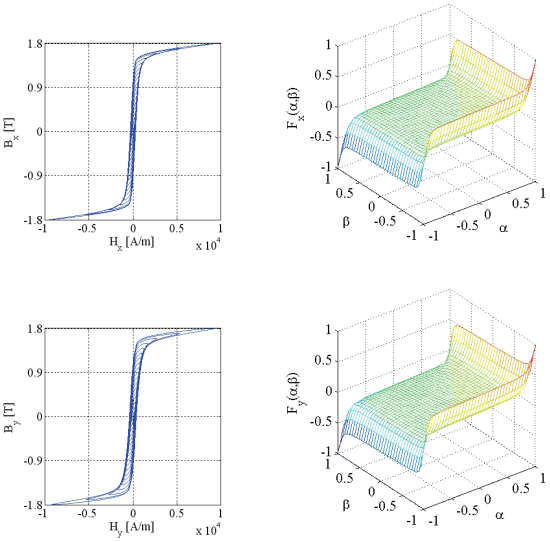

Fig. 2. The concentric minor loops and the Everett functions measured in *x* and *y* directions

The vector Preisach hysteresis model

The vector Preisach model is the superposition of scalar models. First, the implemented scalar model is presented shortly [14], than the Fourier expansion of the measured Everett functions, finally the identification task applying the linearly and circularly polarized measured data is introduced.

The output of the inverse Preisach model, i.e. the magnetic field intensity, can be calculated by a double integral defined over the Preisach triangle [11],

(4) $$H(t)=\iint_{\alpha\ge\beta}\mu(\alpha,\beta)\gamma(\alpha,\beta,B(t))\,\mathrm{d}\alpha\,\mathrm{d}\beta\ ,$$

where $\mu(\alpha,\beta)$ is the distribution function determined from measurements, and $\gamma(\alpha,\beta,B(t))$ is the characteristics of one elementary hysteron, and $B(t)$ is the magnetic flux density, i.e. the input of the model. The variables α and β are called switching fields of the rectangular hysteron.

The realization in (4) results in a time consuming algorithm because of the operation of the double integral. A much faster method can be investigated by the use of the above presented Everett function $F(\alpha,\beta)$, since it is the double integral of the distribution function. According to this definition, the output of the model can be calculated by a sum as [11,14]

(5) $$H(t)=H_{\max}\left(-F(\alpha_0,\beta_0)+2\sum_{k=1}^{K}\left[F(\alpha_k,\beta_{k-1})-F(\alpha_k,\beta_k)\right]\right),$$

where α_k and β_k are the increasing and the decreasing sequences of the normalized magnetic flux density inside the sample and stored by using the staircase line, moreover α_0 and β_0 denote the first turning point in the first magnetization curve and *K* is the number of stairs in the staircase line. $H_{\max}$ denotes the maximum value of the magnetic field intensity of the model.

Another practical advantage of the Everett function is the easy measurement of it [11,12,14]. The Everett function is usually obtained from the measured first order reversal curves. However the concentric minor loops are applied here. The Everett function can be calculated as

(6) $$F(\alpha,\beta)=\frac{H_\alpha-H_{\alpha\beta}}{2}\ ,$$

where H_α is the reversal output value of the hysteresis operator on the first magnetization curve corresponding to the input value equal to α. The point (α,H_α) defines the peak value of the input as well as the output. The output $H_{\alpha\beta}$ is according to the input $B=\beta$ on the concentric minor loop starting from the point (α,H_α).

After measurements, the Everett functions have been approximated by a tensor product representation of piecewise cubic Hermite interpolating splines [17].

The vector Preisach model has been constructed as the superposition of scalar models [11], i.e. the magnetic field intensity vector has been obtained as a superposition of continuously distributed scalar models on the two dimensional plane,

(7) $$\boldsymbol{H}(t)=\int_{-\pi/2}^{\pi/2}\boldsymbol{e}_\varphi\,H_\varphi(t)\,\mathrm{d}\varphi=\int_{-\pi/2}^{\pi/2}\boldsymbol{e}_\varphi\,\mathrm{B}\left\{B_\varphi(t)\right\}\mathrm{d}\varphi\ .$$

In computer realization, the magnetic field intensity vector can be approximated by the following sum:

(8) $$\boldsymbol{H}(t)\cong\sum_{i=1}^{n}\boldsymbol{e}_{\varphi_i}\,\mathrm{B}\left\{B_{\varphi_i}(t)\right\}\Delta\varphi\ ,$$

where $\varphi_i=-\pi/2+(i-1)\pi/n$ ($\Delta\varphi=\pi/n$), and *n* is the number of directions. It means that the sum in (5) must be calculated *n* times.

The scalar magnetic flux density in the direction φ_i can be calculated from the two components of the magnetic flux density vector as

(9) $$B_{\varphi_i}=B_x\cos\varphi_i+B_y\sin\varphi_i\ .$$

This results in the well known extension of the scalar hysteresis models [11]. In front of using (9), the following projection can be useful [15,16]:

(10) $$B_{\varphi_i}(w)=B_x\,\mathrm{sign}(\cos\varphi_i)\left|\cos\varphi_i\right|^{1/w}+B_y\,\mathrm{sign}(\sin\varphi_i)\left|\sin\varphi_i\right|^{1/w}.$$

If the parameter *w* is equal to 1, the original extension can be obtained, i.e. the equation (9), however $w>1$ results in the model, which can simulate small anisotropic behaviors in the case of rotational excitation [18].

The two orthogonal components of the magnetic field strength, the two components of the output of the vector model, are finally given by

(11) $$H_x=\sum_{i=1}^{n}H_{\varphi_i}\cos\varphi_i\ ,\quad H_y=\sum_{i=1}^{n}H_{\varphi_i}\sin\varphi_i\ .$$

The measured Everett function is depending on the polar angle φ, and according to (2) and (3), it can be approximated by its Fourier series [13,14],

(12) $F(\alpha,\beta,\varphi) \cong \sum_m F_m(\alpha,\beta)\cos(2m\varphi)$.

Here $F_m(\alpha,\beta)$ are the Fourier coefficients [13,14],

(13) $$F_0(\alpha,\beta) \cong \frac{\Delta\varphi}{\pi}\left(\begin{matrix}F(\alpha,\beta,0)+F(\alpha,\beta,\pi/2)\\ +2\sum_{j=1}^{N-1}F(\alpha,\beta,\varphi_j)\end{matrix}\right)$$

and

(14) $$F_m(\alpha,\beta) \cong \frac{2\Delta\varphi}{\pi}\left(\begin{matrix}F(\alpha,\beta,0)+(-1)^m F(\alpha,\beta,\pi/2)\\ +2\sum_{j=1}^{N-1}F(\alpha,\beta,\varphi_j)\cos(2m\varphi_j)\end{matrix}\right)$$

according to the definition of Fourier coefficients, and the integration has been approximated by the trapezoidal rule. The value of *N* in (13) and (14) is the number of Everett functions approximated by (1), and $\Delta\varphi = \pi/2N$.

By applying the coefficient in (8) and only the first order Fourier coefficient from (9), the measured Everett functions can be approximated with a relative error about $5\cdot10^{-4}$ (this is the maximum value). The applied Fourier coefficients can be seen in Fig. 3. The coefficient $F_0(\alpha,\beta)$ has the usual shape, but $F_1(\alpha,\beta)$ has no got physical meaning.

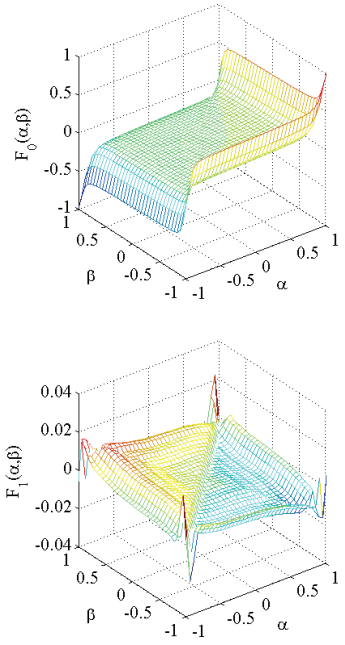

Fig. 3. The Fourier coefficients of the measured Everett functions

The representation of the φ-dependent measured Everett function by two Fourier coefficients $F_0(\alpha,\beta)$ and $F_1(\alpha,\beta)$ means that the output of the anisotropic vector hysteresis model must be the superposition of two vector hysteresis sub-models according to $F(\alpha,\beta,\varphi) \cong F_0(\alpha,\beta)+F_1(\alpha,\beta)\cos(2\varphi)$ (see (12)). The Everett function-like coefficients $F_0(\alpha,\beta)$ and $F_1(\alpha,\beta)$ must be identified by the following scheme.

The identification is based on the following integral equation [10,11,13]:

(15)
$$F_m(\alpha,\beta) = \int_{-\pi/2}^{\pi/2} \cos\varphi\cos(2m\varphi)\, E_m(\alpha\cos^{1/w}\varphi, \beta\cos^{1/w}\varphi)\,\mathrm{d}\varphi ,$$

where $E_m(\alpha,\beta)$ are the unknown Everett functions, which can be identified by a lengthy algorithm [10]. Here $E_m(\alpha,\beta)$ is depending on the value of *w* which is the parameter determined by applying measured data of rotational magnetization process.

According to $F_0(\alpha,\beta)$ and $F_1(\alpha,\beta)$, $E_0(\alpha,\beta)$ and $E_1(\alpha,\beta)$ are the two unknown Everett functions. Parameter *w* can be different for different *m*, denoted by *w* and *q* if $m=0$, and $m=1$, respectively, resulting two degree of freedom.

The identification process is the following:

1. Starting with $w=1$, $q=1$.
2. Identify $E_m(\alpha,\beta)$ according to (15) by applying $F_m(\alpha,\beta)$.
3. Simulate some circular magnetization process by applying the superposition of the two vector hysteresis characteristics ($m=0,1$) according to $E_0(\alpha,\beta)+E_1(\alpha,\beta)\cos(2\varphi)$ and the parameter *w* and *q* in (10).
4. Modify the parameters *w* and *q* according to the difference between the measured and the simulated circular data. This algorithm is based on the Nelder-Mead Simplex Method [19]. Step back to 2. until the difference between measured and simulated circular loops is not small enough.

The optimal value of the parameters are: $w=1.1070$, $q=1.1786$, the number of directions in one vector model is $n=28$.

Comparison between measured and simulated data

The identified model has been tested by comparing measured and simulated data (Fig. 4 and Fig. 5). The measured and simulated curves are in a very good agreement in the linear as well as in the rotational magnetization process.

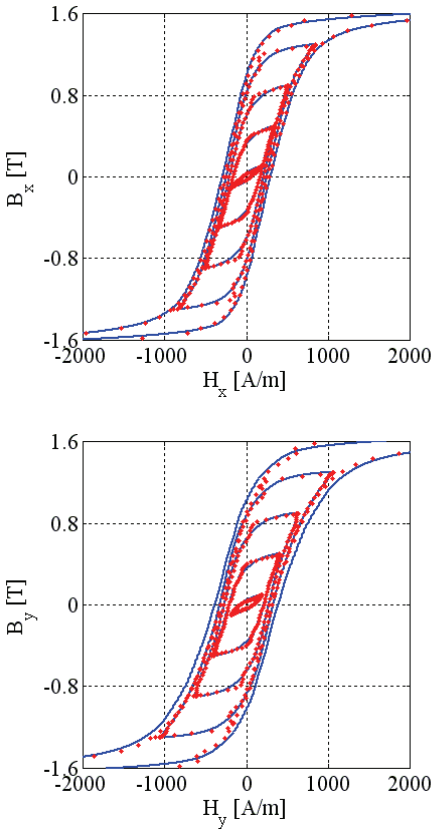

Fig. 4. Comparison between measured (solid line) and simulated (dotted line) hysteresis curves in the *x* and *y* directions

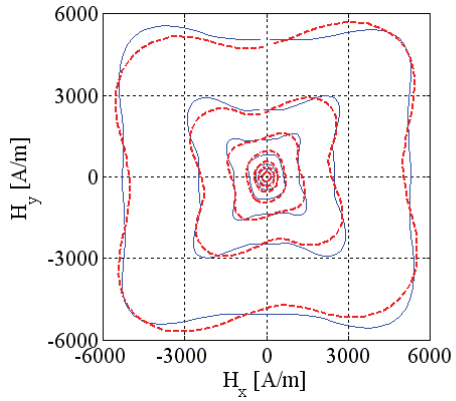

Fig. 5. Comparison between measured (solid line) and simulated (dashed line) magnetic field intensity when controlling circular flux density in the counter-clockwise direction

Conclusion

The isotropic vector Preisach model has been modified by introducing a new parameter *w* which can be identified by using measured data from circular magnetization process. The behavior of the resulting isotropic model is closer to the real magnetization schemes. Here, a generalization of this kind of model has been introduced. The measured Everett functions are different in the different directions which can be handled by the technique of Fourier series. Different value of the parameter *w* has been used in the case of different Fourier coefficients to reach more degree of freedom. The new model is able to take the uniaxial properties into account as well as the rotational process.

Acknowledgements: This paper was supported by the János Bolyai Research Scholarship of the Hungarian Academy of Sciences (BO/00064/06), by Széchenyi István University (15-3210-02), by the Hungarian Scientific Research Fund (OTKA PD 73242). The author would like to thank Prof. Laurentiu Stoleriu ("Al. I. Cuza" University, Iasi, Romania) for the discussions while developing the measurements.

REFERENCES

[1] Cardelli E., Faba A., Vector Hysteresis Measurement Via a Single Disk Tester, *Physica B*, 372 (2006), 143-146.
[2] Jesenik M., Gorican V., Trlep M., Hamler A., Stumberger B., Field homogenity in a twophase round rotational single sheet tester with one and both side shields, *Jour. of Magn. and Magn. Mat,* 254−255 (2003), 247−249.
[3] Makaveev D., Rauch M., De Wulf M., Melkebeek J., Accurate field strength measurement in rotational SST, *Jour. of Magn. and Magn. Mat,* 215−216 (2000), 673−676.
[4] Ragusa C., Fiorillo F., A three-phase single sheet tester with digital control of flux loci based on the contraction mapping principle, *Jour. of Magn. and Magn. Mat,* 304 (2006), 568−570.
[5] Jesenik M., Gorican V., Trlep M., Hamler A., Stumberger B., Field homogenity in a 2-phase rotational SST with square sample, *IEEE Trans. on Magn,* 39 (2003) 1495-1498.
[6] Belkasim M., *Identification of loss models from measurements of the magnetic properties of electrical steel sheets*, MSc Thesis, 2008, http://lib.tkk.fi/Dipl/2008/urn012787.pdf.
[7] Guo Y., Zhu J. G., Zhong J., Lu H., Jin J. X., Measurement and Modeling of Rotational Core Losses of Soft Magnetic Materials Used in Electrical Machines: A Review, *IEEE Trans. on Magn,* 44 (2008), 279-291.
[8] Fonteyn K., Belahcen A., Arkkio A., Properties of Electrical Steel Sheets Under Strong Mechanical Stress, *Pollack Periodica,* 1 (2006), 93-104.
[9] Kuczmann M., Design of 2D RRSST system by FEM with ***T***,Φ-Φ potential formulation, *Pollack Periodica*, 3 (2008), 67-80.
[10] Kuczmann M., Measurement and simulation of vector hysteresis characteristics, *IEEE Trans. on Magn,* 45 (2009), 5188-5191.
[11] Mayergoyz I. D., *Mathematical models of hysteresis,* Springer, New York, 1991.
[12] Della Torre E., *Magnetic hystereis*, IEEE Press, New York, 1999.
[13] Ragusa C., Repetto M., Accurate analysis of magnetic devices with anisotropic vector hysteresis, *Physica B,* 275 (2000), 92−98.
[14] Kuczmann M., Iványi A., *The finite element method in magnetism*. Akadémiai Kiadó, Budapest, 2008.
[15] Adly A. A., Mayergoyz I. D., A new vector Preisach-type model of hysteresis, *J. Appl. Phys,* 73 (1993), 5824-5827.
[16] Dlala E., Belahcen A., Katarzyna A. F., Belkasim M., Improving loss properties of the Mayergoyz vector hysteresis model, *IEEE Trans. on Magn,* 46 (2010), 918-921.
[17] Fritsch F. N., Carlson R. E., Monotone Piecewise Cubic Interpolation, *SIAM J. Numerical Analysis*, 17 (1980), 238-246.
[18] Enokizono M. (ed.), *Two-Dimensional Magnetic Measurement and its Properties*, JSAEM Studies in Applied Electromagnetics, 1, Oita, Japan, 1992.
[19] Lagarias J., Reeds J. A., Wright M. H., Wright P. E., Convergence Properties of the Nelder-Mead Simplex Method in Low Dimensions, *SIAM J. of Opt.,* 9 (1998), 112-147.

***Authors**: Dr. Miklós Kuczmann, PhD, Széchenyi István University, Department of Telecommunications, Laboratory of Electromagnetic Fields, Egyetem tér 1, H-9026 Győr, Hungary, E-mail: kuczmann@sze.hu.*